Cladding Breaches in a Fast Reactor Mixed-Oxide Fuel Assembly

U.P. Nayak, P.J. Levine, A. Boltax
Westinghouse Electric Corporation, Advanced Reactors Division, P.O. Box 158, Madison, Pennsylvania 15663, U.S.A.

Summary

Cladding breaches occurred in a grid-type mixed-oxide fuel assembly (WSA-8) irradiated in EBR-II to 10.7% burnup and 9.2×10^{22} n/cm^2 (E 0.1Mev) fluence. The cladding breaches were found in two adjacent fuel pins with 20% cold-worked titanium-modified AISI 316 stainless steel near the top of the fuel column. The irradiation history of the fuel pin assembly involved an initial 11,376-hour irradiation at a peak linear power of 39 kW/m with start-of-life and time-averaged cladding midwall temperatures of 675°C and 625°C, respectively. Following an interim examination at 10.6% burnup and reconstitution, the assembly operated for 239 hours with cladding temperatures increased to start-of-life values, at which time the cladding breaches occurred. The breached pins exhibited large local deformations in the vicinity of the breaches with no associated void swelling. The cladding microstructures at the breach sites were typical of high-temperature creep rupture with associated creep voids. The cause of the cladding breaches is believed to be due to a local hot spot associated with extensive bow of a peripheral pin and subsequent reorientation of the bow during removal and insertion of the adjacent pin at the time of the interim examination.

1. Introduction

The WSA-8 mixed-oxide fuel experiment was designed to study the comparative behavior of three types of 20% cold-worked claddings under nominally identical conditions. The cladding materials included AISI 316, AISI 321 and titanium-modified AISI 316 stainless steels. A grid-spaced vehicle was used in the experiment to eliminate any possible pin-to-pin interactions. Details of the grid-spaced assembly and fuel pin design have been described previously [1]. The assembly was irradiated in EBR-II for 11,376 effective full power hours at a peak linear power of 39 kW/m to a peak burnup and fluence of 10.6% and 9.1×10^{22} n/cm^2 (E>0.1Mev), respectively, prior to interim discharge. At the interim discharge, several fuel pins were removed for destructive examination, results of which have been published [2]. The assembly was reconstituted as a run-to-cladding-breach (RTCB) assembly, omitting pins with AISI 321 cladding, and the irradiation was continued with a resized coolant inlet orifice to obtain substantially higher cladding temperature. A typical set of calculated power and cladding ID temperature histories for one of the peak pins is illustrated in Figure 1.

Cladding breach was detected after 239 hours of additional irradiation and the assembly was discharged. Subsequently, two adjacent pins, one peripheral and one interior, with titanium modified AISI 316 cladding were identified as breached pins based on ^{133}Xe gamma scan results.

2. Post-Irradiation Examination Results

Visual examination of the fuel pins did not conclusively identify the breached region. One of the breached pins, W8-57, was removed from the grid-spaced inner duct bundle during interim examination and reinserted for irradiation in the RTCB test. The surface of this pin revealed extensive scratching caused by withdrawal and reinsertion. Numerous minute cracks in the cladding in a 50-mm region at the top of the fuel column were also observed. Pin pressurization while immersed in alcohol was used to identify the breached region.

Diametral strain profiles are illustrated in Figures 2 and 3 for the AISI 316 and titanium-modified AISI 316 claddings, respectively. The AISI 316-clad fuel pins showed a single peak in the strain profile, $\sim$2% $\Delta D/D$, slightly above the core midplane. The strain profile was not affected by the RTCB operation. The titanium-modified AISI 316-clad fuel pins showed a low temperature peak, $\sim$2% $\Delta D/D$ at an X/L of 0.2 to 0.4, and a high temperature peak at an X/L of 0.9. Prior to RTCB operation, only the interior fuel pins, which operated at a slightly higher temperature than the peripheral pins, exhibited a small second peak. After the RTCB operation most of the pins showed the second peak, the magnitude being approximately proportional to the temperature. The two breached pins showed much larger hot end diametral strains.

A comparison of the post-breach and interim diametral strain profiles of pin W8-57, illustrated in Figure 4, revealed that the peak strain at the hot end increased from 1.1% $\Delta D/D$ at the interim to 3.6% $\Delta D/D$ after the RTCB operation. The additional strain occurred in 239 effective full power hours. A similar comparison for a comparable AISI 316-clad pin showed little change in diametral strain.

Peak swelling of 4.9% $\Delta V/V_o$ at an X/L of 0.3 was determined from immersion density measurements on the W8-57 pin. In the breached region, the measured swelling was less than 0.25% $\Delta V/V_o$, indicating that the large strain was not caused by enhanced swelling of the

cladding. Comparative total strain and swelling profiles for pin W8-57 are illustrated in Figure 5.

Microstructural examination of fuel and cladding indicated that breach occurred ~40 mm below the top of the fuel column in pins W8-37 and -57. The breaches had the characteristics of a high-temperature creep rupture. Figure 6 shows a transverse cross section at the breach region of pin W8-57. The as-polished and etched cladding structures are illustrated in Figure 7. The as-polished cladding shows the breach and associated creep voids. The etched structures showed a considerable amount of second phase precipitation, indicating that high temperatures were experienced during operation. Cladding structures diametrically opposite the breach showed less second phase precipitation, indicating lower temperatures than the breach region during irradiation. Figure 8 shows cladding structures at two different azimuthal orientations in the same axial section of pin W8-37.

The cladding structures did not show any evidence of recrystallization. Microhardness values near the breach ranged from 200 to 212 DPH compared to values of 260 DPH in a diametrically opposite region. Cladding thickness measurements on transverse sections revealed localized thinning, ~20% of the original thickness, in the vicinity of the breaches.

A longitudinal cladding section from pin W8-57, taken from a region above the breach, was metallographically examined to evaluate the extent of second phase precipitation. The volume of second-phase precipitate in the same azimuthal orientation as the breach was less than that at the breach vicinity, indicating that the temperature in the downstream region was lower than that in the vicinity of the breach.

2. Discussion and Evaluation of Results

The breached pins, W8-37 and -57, were adjacent to each other in the assembly, the former in a peripheral position and the latter in an interior position. The breaches were observed at the same axial locations with associated large strains and azimuthal temperature variations were observed in both pins. In addition, the titanium-modified 316 clad pins exhibited a second cladding strain peak at the hot end, which was not associated with cladding swelling. These observations lead to a conclusion that the cause of the breach was a localized hot spot due to coolant flow reduction in a common flow channel. The breach locations was ~6 mm below the grid supports. The large bow (>4 cm) in pin W8-37 and removal and reinsertion with possible reorientation of pin W8-57 may have caused a reduction in coolant channel area giving rise to the hot spot. The hot spot was very localized, since cladding structures ~25 mm above the breach (downstream) showed evidence of lower cladding temperatures.

Analysis of a typical pin in the WSA-8 RTCB assembly with the LIFE-3 [3] code indicated a very low probability of cladding breach before 2900 hours of RTCB operation, based on stress rupture data at nominal cladding temperatures. Since the cladding breach occurred after 239 hours of operation, an analysis was performed to determine the increase in cladding temperature required to be consistent with cladding breach at the observed time. The results of the analysis, illustrated in Table I, indicate that a cladding temperature increase of 90°C could give rise to the cladding breach. An evaluation of the thermal hydraulic uncertainty for the irradiation assembly showed the 3σ uncertainty to be 104°C. The second-phase precipitate volume measurements and the incremental creep strain of 2.5% in the final 239 hours of operation were also consistent with local cladding temperatures in excess of 700°C.

Comparison of the cladding strain behavior of the 316 and titanium-modified 316 (Figures 2, 3 and 4) indicates a greater sensitivity of the modified alloy to the cladding temperature increase during RTCB operation. This sensitivity is believed to be related to the differences in composition of the two alloys, particularly the titanium and silicon as shown in Table 2. The breached pins exhibited the greatest dimensional instability which is consistent with the conclusion that they experienced a local hot spot.

References

[1] LEVINE, P. J. and SCHWALLIE, A. L., "Experimental Grid-Type Subassemblies for Irradiation in EBR-II," in Proceedings of Conference on Irradiation Experimentation in Fast Reactors, Jackson, WY, September, 1973.

[2] LEVINE, P. J., NAYAK, U. P., SCHWALLIE, A. L. and BOLTAX, A., "Irradiation Performance of WSA-3, -4 and -8 Mixed-Oxide Fuel Pins in Grid-Spaced Assemblies," International Conference on Fast Breeder Reactor Fuel Performance, Monterey, California, March, 1979.

[3] STEPHEN, J. D., BIANCHERIA, A. and BILLONE, M. C., "The LIFE Code System for Analysis of Oxide Fuel Pin Thermal/Structural Behavior," Advanced LMFBR Fuels, J. A. Leary and J. H. Kittel, ERDA 4455, 1977.

TABLE I

WSA-8 RTCB Cladding Breach Analysis

Cladding ID Temperature °C	Calculated Time to Breach (Hours) at 50% Probability*		
	One Pin	10 Pins	30 Pins
679 (Nominal)	7000	3500	2900
729	1600	800	600
769	500	250	200

*Effective full power hours (EFPH) following 11,376 EFPH of initial operation.

TABLE II

Chemical Composition (Wt. %) of Cladding Materials

Element	AISI 316 (N-lot)	Titanium-Modified AISI 316
C	0.053	0.054
Mn	1.41	1.41
P	0.011	0.024
S	0.006	0.007
Si	0.50	0.011
Cr	15.99	16.65
Ni	13.27	14.01
Mo	2.16	2.29
Cu	0.07	0.06
Ti	----	0.22
N	0.012	0.0005
Fe	BAL	BAL

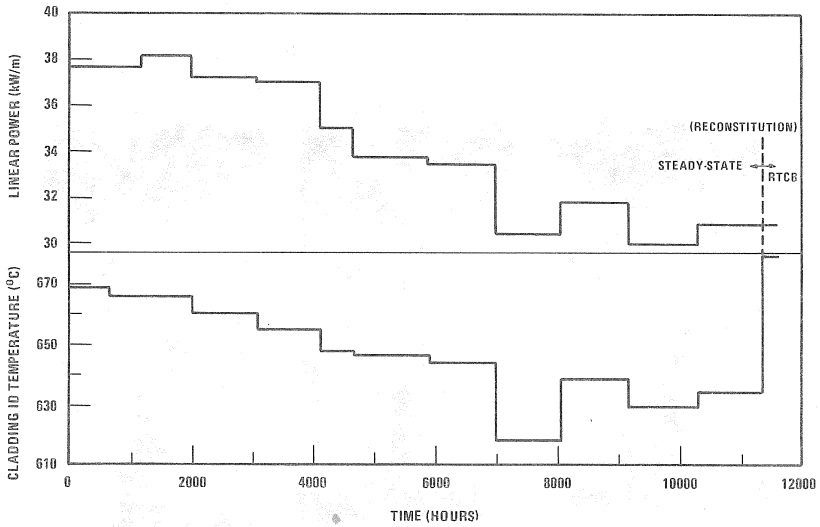

FIGURE 1. Power and Temperature History for Pin W8-45

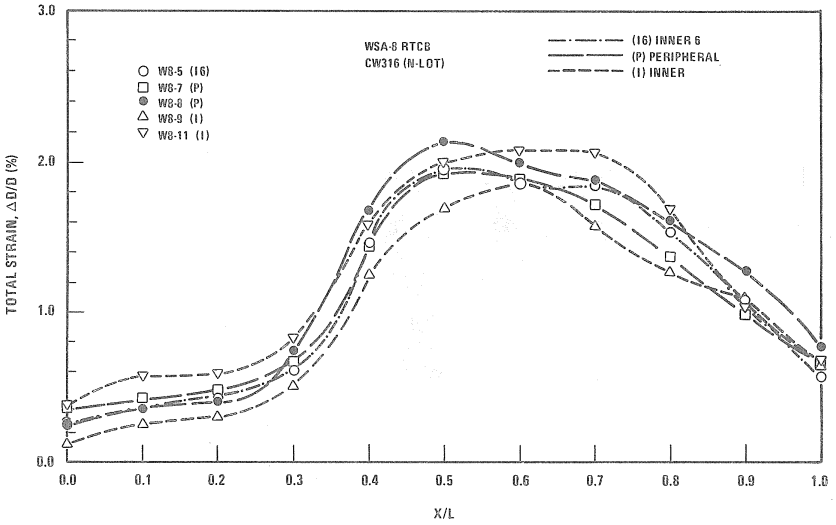

FIGURE 2. Diametral Strain Profiles of WSA-8 RTCB Fuel Pins with AISI Type 316 (N-Lot) Cladding

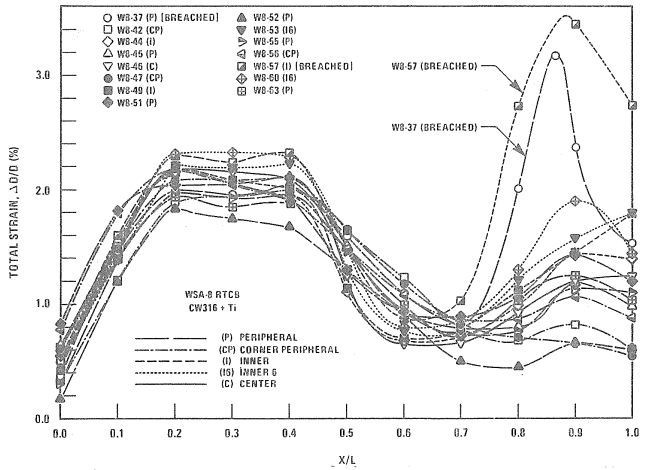

FIGURE 3. Diametral Strain Profiles of WSA-8 RTCB Fuel Pins with Titanium-Modified AISI Type 316 Cladding

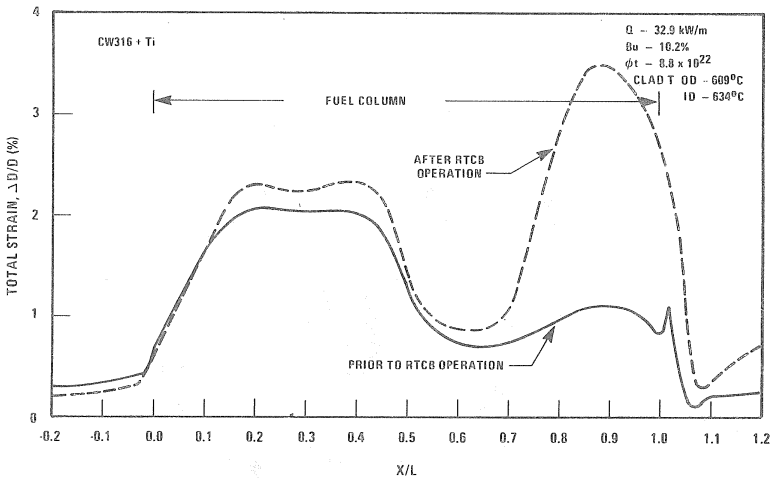

FIGURE 4. Diametral Strain Profiles of Pin W8-57

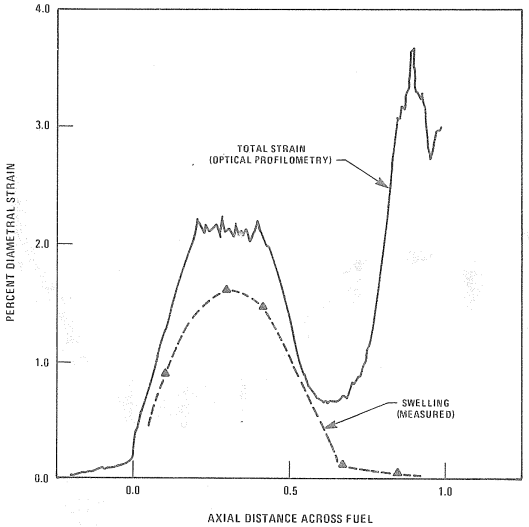

FIGURE 5. Total and Swelling Strains of Pin W8-57

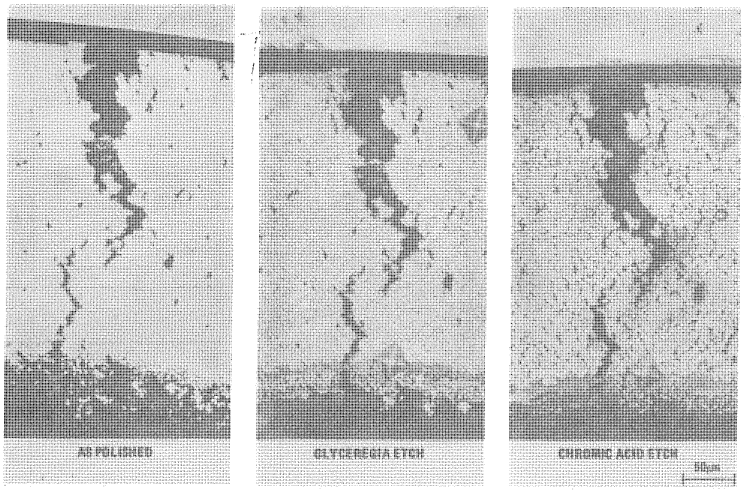

FIGURE 7. Cladding Structure at the Breach in Pin W8-57

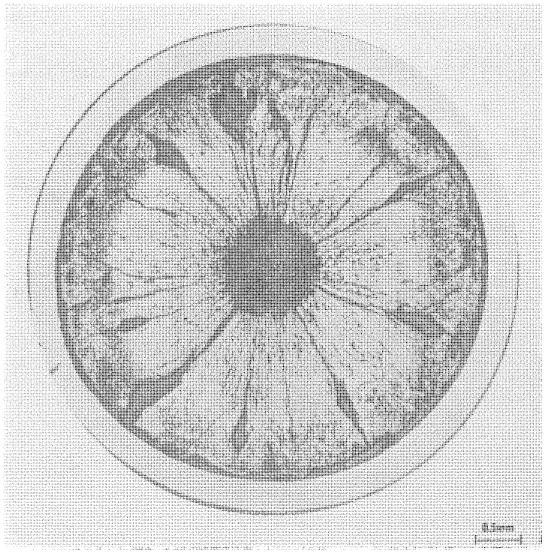

FIGURE 6. Transverse Section From Pin W8-57 at the Breached Region (X/L=0.89)

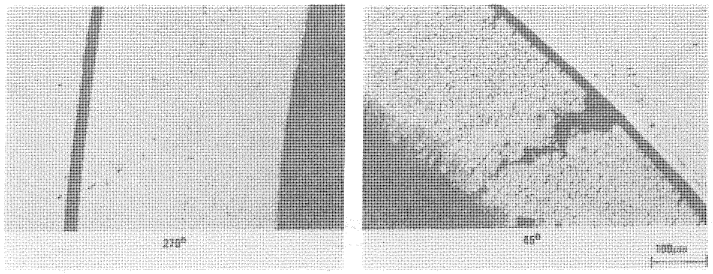

FIGURE 8. Cladding Structures at Breached Section in Pin W8-37 (Chromic Acid Etch)